Solid State Communications (2016) 1–4

Contents lists available at ScienceDirect

Solid State Communications226

journal homepage: www.elsevier.com/locate/ssc

First-principles calculations of properties for chalcogen (S, Se, Te) doped silicon

Lingyan Du [a,b], Zhiming Wu [a], Shibin Li [a,*], Zheng Hu [a], Yadong Jiang [a]

[a] School of Optoelectronic Information, State Key Laboratory of Electronic Thin Film and Integrated Devices, University of Electronic Science and Technology of China, Chengdu 610054, PR China

[b] School of Automation and Electronic Information, Sichuan University of Science & Engineering, Zigong, Sichuan 643000, PR China

ARTICLE INFO

Article history:
Received 23 July 2015
Received in revised form
30 October 2015
Accepted 6 November 2015
Accepted by Ralph Gebauer
Available online 14 November 2015

ABSTRACT

In this paper, density-functional theory based methods are utilized to systematically investigate the properties of chalcogens (S, Se, Te) doped silicon at different doping concentration. The calculated crystal structures indicate that Se-implanted Si at concentration of 1.56% show minimum lattice distortion and formation energy. Intermediate band caused by introduction of chalcogen impurities is beneficial to strong optical absorption in the infrared range. The calculations carried out demonstrate that energy band structure and optical absorption coefficient are all associated with the doping concentration. The bandwidth of intermediate band and forbidden energy gap are broadened due to the increase of impurities concentration. The dependence of optical absorption on doping concentration is confirmed by the calculations. The results reveal that S/Se/Te-doped silicon at concentration on the order of 1.04% is probably suitable candidate for intermediate band materials.

1. Introduction

Silicon is well known as the most commonly used material in photoelectric field. However, the band gap of crystalline silicon limits its application at wavelength longer than 1100 nm. Recently, intermediate band (IB) materials derived from Si are reported as a promising candidate for development of infrared photo-detector and solar cell [1–3]. A proposed method for obtaining IB materials is introducing impurities in semiconductor [4], owing to the deep level impurities are beneficial for absorbing low energy photons [5]. Transition metals such as chalcogens (S, Se, Te) have been chosen as the donor impurities in fabricating of black silicon. chalcogens-doped Si have been fabricated by different kinds of experimental methods, for example, laser irradiation on Si surface in the atmosphere of gas such as SF_6, femtosecond laser irradiation on Si with chalcogens thin-film, or ion implantation followed by irradiation with laser pulse [6,7]. All the experimental results show that S/Se/Te-doped Si has high absorption in near-infrared range. The origins of these phenomena have been studied using the density functional theory (DFT) in recent reports [8–10]. Sánchez et al. calculated the energetic properties of chalcogens-doped Si and reached a conclusion that chalcogens-doped Si show strong optical absorption in the infrared range [9]. Zhao et al. studied the insulator-to-metal transition of sulfur-doped Si with the increase of sulfur concentration [10]. Our group has fabricated micro-pyramids and nano-pores structures on the silicon surface by metal-assisted wet chemical etching, the absorption ratio at wavelengths longer than 1.1 μm was raised [11–13]. However, there is limited report about theoretical analysis of the influence of doping concentration on impurity formation energy, energetic properties and optical properties.

In this paper, the models used to simulate chalcogens-implanted Si on different doping level are proposed. Afterward, the crystal structural, energetic, and optical properties are investigated. The results indicate the obvious dependence of energetic and optical properties of chalcogens-doped silicon on doping concentration.

2. Calculation methods

Density-functional theory (DFT) combined with plane-wave ultra-soft pseudo-potential [14,15] calculations were carried out to study the properties of the pure and S/Se/Te-doped silicon. The cells used in this study were derived from various sizes of cubic super cell of crystalline Si: $2\times2\times2$ (Si_{64}), $2\times2\times3$ (Si_{96}), and $3\times3\times3$ (Si_{216}). The method of atomic substitution was used to construct doping models, in the case three different super cells represented different doping concentration at 1.56%, 1.04%, 0.46% respectively. This approach works on the premise that impurities

* Corresponding author. Tel.: +86 13684308845.
E-mail addresses: dulingyan927@163.com (L. Du), shibinli@uestc.edu.cn (S. Li).

http://dx.doi.org/10.1016/j.ssc.2015.11.006
0038-1098/

have uniform distribution in the silicon host. However, in a real system, impurities distribution may be in disorder, the lattice parameters and bond lengths between Si and chalcogen atoms no longer have periodicity in that case. The atomic interactions are also different from the description in this paper. Taking into account the characteristics of optoelectronic devices, our research group is looking for a new experimental method to achieve uniform doping.

All Geometry Optimization and energy calculations were carried out with CASTEP code [15]. The generalized gradient approximation (GGA) through the PBE functional was used for the exchange-correlation potential [16]. The maximum plane-wave energy cutoff was 280 eV, energy calculations were completed in the reciprocal space, and a $4\times4\times4$ Monkhorst–Pack grid of **k**-points was used to sample the first irreducible Brillouin zone. In our calculations, set thresholds of 0.01 eV/Å for the inter-atomic forces and 0.02 GPa for the lattice stress, the maximum displacement was set for 5.0×10^{-4} Å. The convergence precision of self-consistent-filed was finally reduced to 5.0×10^{-7} eV/atom. The minimization algorithm was chosen the Broyden–Fletcher–Goldfarb–Shanno (BFGS) scheme [17].

The optical properties were studied by dielectric function, $\varepsilon(\omega)=\varepsilon_1(\omega)+i\varepsilon_2(\omega)$. The imaginary part can be calculated independently based on Eq. (1), and the real part was obtained from the imaginary part using the Kramers–Kronig relation based on the equation. Consequently, the optical absorption coefficient would be calculated [18,19].

$$\epsilon_2(\omega)=\frac{4\pi^2}{m^2\omega^2}\sum_{V,C}\int_{BZ}d^3k\frac{2}{(2\pi)}|eM_{CV}(K)|^2\cdot\delta\left[E_C(k)-E_V(k)-h\omega\right] \quad (1)$$

$$I(\omega)=\sqrt{2}\omega[\sqrt{\varepsilon_1^2(\omega)+\varepsilon_2^2(\omega)}-\varepsilon_1(\omega)]^{1/2} \quad (2)$$

3. Results and discussions

3.1. Structure properties

In the super cell of crystalline Si, one Si atom is replaced by one S/Se/Te atom, following, the atomic structure of doped Si with formula Si_nX is optimized, in which X indicates S/Se/Te. The optimized cell constants are calculated by using exchange-correlation function [16] and corresponding results are shown in Table 1. The chalcogen impurities cause lattice distortion of silicon host. The bond length of Si–X is larger than that of Si–Si in the same model, as well as larger than Si–Si bond length in the pure Si model. The growth of Si–X bond length directly shortens bond length of Si–Si due to doping. The lattice parameters (5.437–5.480 Å) of all chalcogens-doped Si are longer than that of the bulk Si (5.43 Å). In compounds of the S-implanted silicon and Te-implanted silicon, it is obvious that higher doping concentration induced larger lattice distortion than that of lower doping. However, for the Se-implanted silicon, the minimum lattice parameter (5.437 Å) appears at the concentration of 1.56%, indicating an increment of 0.007 Å compared to the pure Si.

The impurity formation energy (E^f) is calculated using Eq. (3) to investigate the chemical stability for existence of chalcogen elements. Where $E[X]$ refers the elemental energy in the most stable form, and the results are listed in Table 1.

$$E^f[Si_nX]=E[Si_nX]-E[X]-\frac{n}{n+1}E\left[Si_{n+1}\right] \quad (3)$$

Usually higher doping concentration and larger atomic radius of impurity mean higher impurity formation energy, but Se-implanted Si does not follow this regularity. In all of the models, $Si_{63}Se$ has the minimum formation energy −15.42 eV. This result implies that the bonding capacity between Se and Si in a certain concentration is stronger than that of S and Te. The minimum bond population of $Si_{63}Se$ is 0.03, indicating that there is ion interaction between Si and Se. The ion-resonance effect increases the bond strength and shortens the bond length. [20]. According to the results above, it can be predicted that Se-implanted Si at the concentration of 1.56% shows better chemical stability compared to other compounds.

3.2. Energetic properties

The electronic band structure and density of states (DOS) that calculated using CASTEP code are presented in Figs. 1 and 2. There is no significant difference among $Si_{63}S$, $Si_{63}Se$ and $Si_{63}Te$, in contrast to the crystalline Si, an intermediate band appears within the Si band gap ascribed to the introduction of donor impurities. Furthermore, compared to the indirect band gap material for pure Si, the VB maximum and the IB minimum of all chalcogens doped Si are located at the same κ-point of Γ, this is conducive to the electronic transition between the two levels. As shown in the figure of DOS, an occupied band appears and all samples fulfill the requirements of an IB material [21]. No obvious difference is observed from the DOS for three types of doping samples at the same doping concentration. Sulfur, Selenium and Tellurium, all these VI elements show some similar energetic properties presented above due to their similar electronic structure.

Brief summaries of the electronic structure for chalogens-doped Si at different doping levels are shown in Tables 2–4. As shown in the Tables, IB widths and forbidden energy gaps are broadened with the increase of impurity concentration. At concentration of 0.46%, the IB widths for all samples are sited at 0.19–0.20 eV, the gaps between VB maximum and CB minimum of all models are larger than 0.6 eV obtained for the pure silicon. The gaps between IB and CB minimum of S/Se/Te-implanted silicon are 0.05 eV, 0.06 eV and 0.05 eV, respectively. When doping

Table 1
Bond length, bond population and impurity formation energy of pure Si and all Chalcogen-doped Si.

Compound	Lattice parameter/Å	Si–X		Si–Si		E^f/eV
		Bond length/Å	Population/e	Bond length/Å	Population/e	
Si(pure)	5.430			2.3663	2.96	
$Si_{63}S$	5.480	2.4461	0.08	2.3651	0.7407	−1.37
$Si_{95}S$	5.465	2.4774	0.08	2.3648	0.7423	−2.30
$Si_{215}S$	5.464	2.4829	0.09	2.3646	0.7471	−3.00
$Si_{63}Se$	5.437	2.5235	0.03	2.3493	0.7467	−15.42
$Si_{95}Se$	5.471	2.5532	0.03	2.3648	0.7436	−1.47
$Si_{215}Se$	5.467	2.5462	0.04	2.3644	0.7474	−1.87
$Si_{63}Te$	5.479	2.6879	0.11	2.3647	0.7316	2.35
$Si_{95}Te$	5.478	2.6972	0.11	2.3644	0.7372	1.44
$Si_{215}Te$	5.470	2.6972	0.13	2.3643	0.7444	1.35

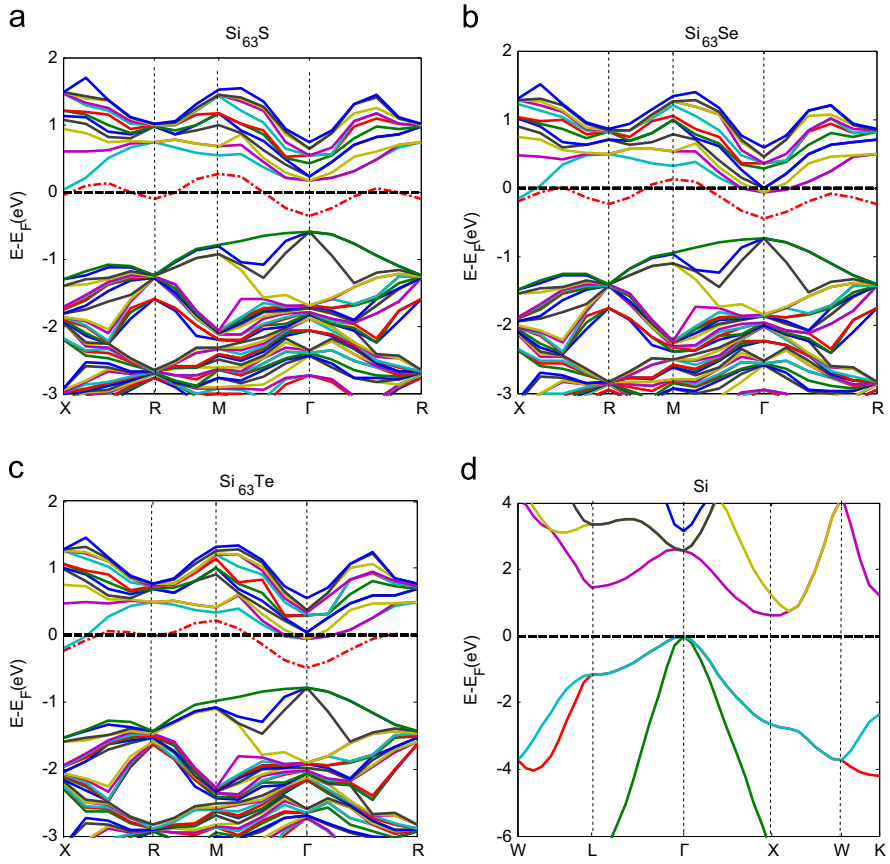

Fig. 1. The electronic band structure for (a) $Si_{63}S$ (b) $Si_{63}Se$ (c) $Si_{63}Te$ (d) Si.

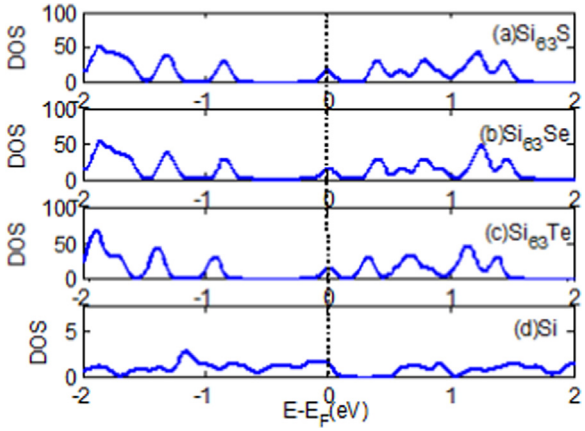

Fig. 2. Density of states for (a) $Si_{63}S$ (b) $Si_{63}Se$ (c) $Si_{63}Te$ (d) Si.

Table 2
Summary of the bandwidth and forbidden energy gaps of the compounds of the S-implanted Si. All values are given in eV.

Compound	IB band width	ΔE [VB–IB]	ΔE [IB–CB]	ΔE [VB–CB]
$Si_{215}S$	0.19	0.44	0.05	0.68
$Si_{95}S$	0.22	0.46	0.11	0.8
$Si_{63}S$	0.23	0.59	0.16	0.98

concentration is increased to 1.04%, the IB widths rise to about 0.22 eV, and the gaps between VB maximum and CB minimum are broadened. The increment of IB width would be slightly reduced in the case of doping concentration at 1.56%. But there is large increase in the width between IB and CB minimum. As a result,

Table 3
Summary of the bandwidth and forbidden energy gaps of the compounds of the Se-implanted Si. All values are given in eV.

Compound	IB band width	ΔE [VB–IB]	ΔE [IB–CB]	ΔE [VB–CB]
$Si_{215}Se$	0.19	0.46	0.06	0.71
$Si_{95}Se$	0.23	0.50	0.13	0.86
$Si_{63}Se$	0.24	0.60	0.16	1.00

Table 4
Summary of the bandwidth and forbidden energy gaps of the compounds of the Te-implanted Si. All values are given in eV.

Compound	IB band width	ΔE [VB–IB]	ΔE [IB–CB]	ΔE [VB–CB]
$Si_{215}Te$	0.20	0.52	0.05	0.77
$Si_{95}Te$	0.22	0.60	0.08	0.88
$Si_{63}Te$	0.22	0.70	0.10	1.02

more high energy photons are absorbed as the bandwidth becomes wider. Accordingly, the absorption of low energy photons is hindered as the bandwidth is widened to a certain extent.

3.3. Optical properties

The introduction of chalogen impurities form impurity bands and change energetic properties, while the energetic properties of different kinds of substitutions at the same doping level are strikingly similar. As promising materials for photoelectric detection and photovoltaic device, the optical properties of S/Se/Te-implanted Si are particularly important. The calculated absorption coefficients of Si_nS, Si_nSe and Si_nTe are illustrated and compared to that of pure Si in Fig. 3. According to the figure, all of chalcogens-doped Si show optical

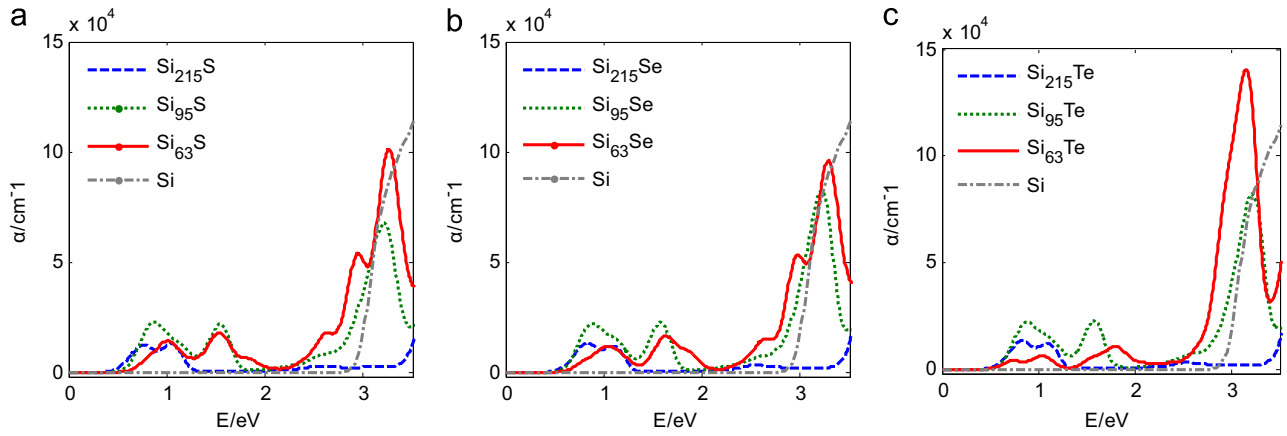

Fig. 3. Optical absorption coefficients of (a) Si_nS (b) Si_nSe (c) Si_nTe.

absorption of photons with energies below the band gap of Si. In the wave range from 0.5 eV to 1.2 eV, the absorption coefficients rise considerably with increasing impurities concentration from 0.46% to 1.04%. However, the absorption descends in this range when impurities concentration further is increased to 1.56%. In the short-wave direction, the absorption increase obviously with the increase of doping concentration, but the variation of absorption in this range does not influence the performance of device which works in infrared and visible. The absorption coefficient varies depending on different doping level can be explained by the energetic properties. Previous literature has reported that absorption of low energy photons below 2 eV is associated with the electronic transitions from the IB to the lowest energy level of the CB, while absorption of high energy photons is associated with the electronic transitions from the VB maximum to CB minimum [9]. The gap between IB and CB minimum is relatively narrow at lower doping level, so there is little optical absorption of photons from 1.2 eV to 2 eV for chalcogens-doped Si at concentration of 0.46%. The gap becomes wider as the doping concentration is increased to 1.04%, this is conducive to the electronic transition thereby increasing the absorption of low energy photons. IB width and forbidden energy gap further become wider as the doping concentration is increased to 1.56%, absorption of photons below 2 eV does not increase, but the absorption of photons above 2 eV rise with increasing doping level.

Related experiments confirmed that the S/Se/Te-implanted Si shows 90% absorption at wavelength from 1100 nm to 2500 nm [2], but crystalline Si exhibits below 15% in the same wave range. The increase in optical absorption is ascribed to the light-trapping because of surface roughness, absorption of medium and intermediate band generated by the introduction of impurities. All of these, only the intermediate band is beneficial for photon-generated carrier. From the results obtained above, it is concluded that doping concentration matters intermediate band and optical absorption, and the strongest absorption in infrared and visible region appears at concentration close to 1.04%.

4. Conclusions

Summarizing, the properties of chalcogens-doped silicon were calculated based on DFT to investigate dependence of energetic and optical properties of them on doping concentration. The calculated lattice distortion and impurity formation energy of S-implanted silicon and Te-implanted silicon rise with increasing impurities concentration. But Se-implanted Si shows minimum lattice distortion and formation energy at concentration of 1.56% because of ion-resonance interactions. Intermediate band appears in the Si band gap because of introduction of S/Se/Te impurities. For compounds of an impurity at different doping level, IB width and forbidden energy gap are broadened with the increase of impurities concentration. All of chalcogens-doped Si show optical absorption of photons with energies between 0.5 eV and 1.2 eV, but the strongest absorption in infrared and visible region appears at concentration close to 1.04%. These findings are helpful to understand previous experimental observations and useful for the design of new experimental materials.

Acknowledgments

The authors would like to acknowledge financial support from the National Natural Science Foundation of China (Grant nos. 61421002, 61204098, and 61371046), Sichuan Province International Scientific and Technological Cooperation and Exchange of Research Plan (Grant no. 2014HH0041) and National Higher-Education Institution General Research and Development Funding (Grant no. ZYGX2014J044).

References

[1] Y. Mo, M.Z. Bazant, E. Kaxiras, Phys. Rev. B 70 (2004) 205210-1–205210-10.
[2] M.A. Sheely, B.R. Tull, C.M. Friend, E. Mazur, Mater. Sci. Eng. B 137 (2007) 289–294.
[3] M.T. Winkler, D. Recht, M.J. Sher, A.J. Said, E. Mazur, M.J. Aziz, Phys. Rev. Lett. 106 (2011) 178701-1–178701-4.
[4] A. Luque, et al., Physica 382B (2006) 320.
[5] M.J. Keevers, M.A. Green, J .Appl. Phys. 75 (1994) 4022.
[6] U. Ikurou, M.W. Jeffery, K. Atsushi, et al., J. Appl. Phys. 113 (2013) 213501.
[7] U. Ikurou, N. Muneyuki, K. Daisuke, et al., Appl. Phys. A 117 (2014) 155–159.
[8] K. Sánchez, I. Aguilera, P. Palacious, et al., Phys. Rev. B 79 (2009) 165203.
[9] K. Sánchez, I. Aguilera, P. Palacious, et al., Phys. Rev. B 82 (2010) 165201.
[10] Z.Y. Zhao, P.Z. Yang., Phys. Chem. Chem. Phys 16 (2014) 17499–17506.
[11] J. Jiang, S. Li, Y. Jiang, Z. Wu, Z. Xiao, Y. Su., J. Mater. Sci.: Mater. Electron. 24 (2013) 463–466.
[12] J. Jiang, S. Li, Z. Xiao, Y. Su, Z. Wu, Y. Jiang., J. Mater. Sci.: Mater. Electron. 24 (2013) 1770–1774.
[13] T. Zhang, P. Zhang, S. Li, et al., Nanoscale Res. Lett. 8 (2013) 351.
[14] K. Lassonen, A. Pasquarello, R. Car, C. Lee, D. Vanderbilt, Phys. Rev. B 47 (1993) 10142.
[15] S.J. Clark, M.D. Segall, C.J. Pickard, P.J. Hasnip, M.J. Probert, K. Refson, M. C. Payne, Z. Krist. 220 (2005) 567–570.
[16] J.P. Perdew, A. Ruzsinszky, G.I. Csonka, O.A. Vydrow, G.E. Scuseria, L. A. Constantin, X. Zhou, K. Burke, Phys. Rev. Lett. 100 (2008) 136406.
[17] B.G. Pfrommer, M. Cate, S.G. Louie, M.L. Cohen, J. Comput. Phys. 131 (1997) 233.
[18] M. Khan, J. Xu, N. Chen, et al., J. Alloy. Compd. 513 (2012) 539.
[19] J. Feng, B. Xiao, J.C. Chen, C.T. Zhou, Y.P. Du, R. Zhou., Solid State Commun. 149 (2009) 1569–1573.
[20] James E. Huheey, Inorg. Chem. (1979).
[21] I. Aguilera, P. Palacious, K. Sánchez, P. Wahnón, Phys. Rev. B 81 (2010) 075206.